OPEN ACCESS

Microbiology ARTICLE

Biosynthesis and characterization of poly(3-hydroxybutyrate-*co*-lactate-*co*-3-hydroxyvalerate) by engineered *Halomonas bluephagenesis*

Jiangnan Chen,[1] Huan Wang,[1] Zhenghao Xu,[1] Yiling Chen,[1] Shi Mu,[1] Shaowei Li,[1] Fuqing Wu,[1,*] Fang Yang,[1,2,*] and Guo-Qiang Chen[1,3,4,5,*]

*Correspondence: chengq@mail.tsinghua.edu.cn (G.C.); yangfang@phabuilder.com (FY); wufuqing@mail.tsinghua.edu.cn (F.W.)

Received: November 14, 2025; Accepted: May 28, 2026; Published Online: June 1, 2026; https://doi.org/10.59717/j.xinn-life.2026.100227

GRAPHICAL ABSTRACT

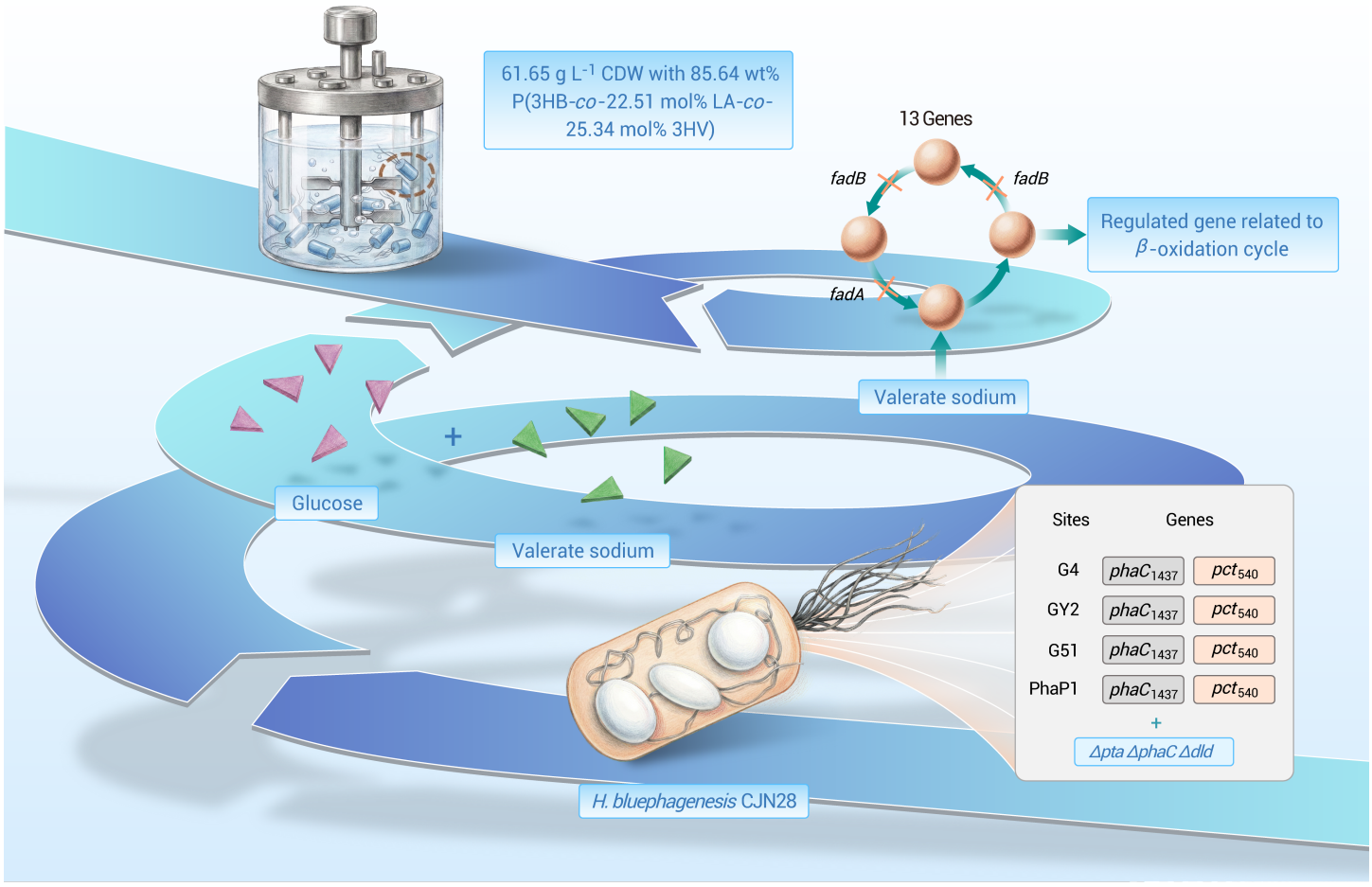

PUBLIC SUMMARY

- Biosynthesis of P(3HB-*co*-LA-*co*-3HV) was achieved in recombinant *Halomonas*.
- Various P(3HB-*co*-LA-*co*-3HV) were produced from glucose and valerate.
- *Halomonas* CJN28 was grown to 62 g L^{-1} CDW containing 86wt% P(3HB-23 mol% LA-25 mol% 3HV).
- Thermal and mechanical properties of various P(3HB-*co*-LA-*co*-3HV) were characterized.

ARTICLE Microbiology

OPEN ACCESS

www.the-innovation.org/the-innovation-life

Biosynthesis and characterization of poly(3-hydroxybutyrate-*co*-lactate-*co*-3-hydroxyvalerate) by engineered *Halomonas bluephagenesis*

Jiangnan Chen,[1] Huan Wang,[1] Zhenghao Xu,[1] Yiling Chen,[1] Shi Mu,[1] Shaowei Li,[1] Fuqing Wu,[1,*] Fang Yang,[1,2,*] and Guo-Qiang Chen[1,3,4,5,*]

[1]School of Life Sciences, Tsinghua University, Beijing 100084, China

[2]PhaBuilder Biotech Co. Ltd., Shunyi District, Zhaoquan Ying, Beijing 101309, China

[3]Center for Synthetic and Systems Biology, Tsinghua University, Beijing 100084, China

[4]Tsinghua-Peking Center for Life Sciences, Beijing 100084, China

[5]MOE Key Lab of Industrial Biocatalysis, Dept Chemical Engineering, Tsinghua University, Beijing 100084, China

*Correspondence: chengq@mail.tsinghua.edu.cn (G.C.); yangfang@phabuilder.com (FY); wufuqing@mail.tsinghua.edu.cn (F.W.)

Received: November 14, 2025; Accepted: May 28, 2026; Published Online: June 1, 2026; https://doi.org/10.59717/j.xinn-life.2026.100227

Citation: Chen J., Wang H., Xu Z., et al. (2026). Biosynthesis and characterization of poly(3-hydroxybutyrate-*co*-lactate-*co*-3-hydroxyvalerate) by engineered *Halomonas bluephagenesis*. *The Innovation Life* **4**:100227.

Halomonas bluephagenesis (*H. bluephagenesis*) was metabolically engineered to efficiently synthesize a biopolymer composed of three monomers—3-hydroxybutyrate (3HB), lactate (LA), and 3-hydroxyvalerate (3HV)—using glucose as the carbon source. In shake-flask cultures with glucose-sodium valerate as the carbon source, the recombinant strain produced 9.48 g L^{-1} of P(3HB-*co*-12.92 mol% LA-*co*-40.48 mol% 3HV). By knocking down 11 genes related to the *β*-oxidation cycle, the composition of the terpolymer was controllable. In a 7-L bioreactor, *H. bluephagenesis* CJN28 reached 61.65 g L^{-1} cell dry weight (CDW containing 85.64 wt% P(3HB-*co*-22.51 mol% LA-*co*-25.34 mol% 3HV). Both *H. bluephagenesis* CJN28 and its cytoskeletal protein MreB-knockdown mutant *H. bluephagenesis* CJN28△*mreB* (exhibiting significant cell enlargement) demonstrated better capability to synthesize P(3HB-*co*-LA-*co*-3HV) when cultured with glucose and gradient concentrations of sodium valerate. Thermal and mechanical studies revealed that the terpolymer exhibited higher ductility compared to P3HB and PLA. This study marks the first attempt of microbial production of P(3HB-*co*-LA-*co*-3HV) with enhanced efficiency for scale up.

INTRODUCTION

The depletion of fossil fuels, unsustainable consumption of resources and plastic pollutions have led to energy crisis and environmental degradation.[1] A potential solution to this global challenge lies in utilizing microbial technology from sustainable feedstocks for the production of industrial chemicals.[2-4] Microorganisms commonly utilized for the biosynthesis of high-value-added products, encompassing a diverse array of chemical compounds and polymers made both by model organisms, exemplified by *Bacillus subtilis*, *Escherichia coli*, *Cupriavidus necator*, yeast and non-model organisms, particularly extremophiles such as *H. bluephagenesis*.[2,5,6]

Polyhydroxyalkanoates (PHA), stored inside bacterial cells as energy reserves, are biodegradable polymers synthesized by microorganisms through the fermentation of glucose or other carbon sources, which is increasingly seen as a sustainable alternative to traditional petroleum-based plastics.[7-10] Increasing the diversity of PHA materials is intended to enhance their application areas.[11] Therefore, studies on biosynthesis of diverse PHA employing the extremophilic *H. bluephagenesis* via next-generation industrial biotechnology (NGIB) have attracted considerable interest and attention.[12]

Currently, representative synthetic PHAs include P(3HB-*co*-3HV) consisting of 3-hydroxybutyrate (3HB) and 3-hydroxyvalerate (3HV), P(3HB-*co*-3HHx) of 3HB and 3-hydroxyhexanoate (3HHx) and P(3HB-*co*-4HB) of 3HB and 4-Hydroxybutyrate (4HB). P(3HB-*co*-3HV) improves the flexibility and processability of PHB by introducing 3HV monomers, achieving higher elongation at break and lower glass transition temperature compared to rigid PLA.[13] The incorporation and modulation of the medium-chain-length monomer 3HHx in P(3HB-*co*-3HHx) enable the copolymer to retain the high strength typical of PHB-based materials while significantly enhancing flexibility and processability, thereby effectively overcoming the inherent brittleness of PHB and the excessive stiffness and limited toughness of PLA.[14] P(3HB-*co*-4HB) offers a tunable combination of high toughness, elasticity, and thermal stability within a fully biodegradable system. By varying the 4HB content, it effectively overcomes the brittleness of PHB and the stiffness of PLA, filling a key gap in flexible and impact-resistant bioplastics.[15]

P(3HB-*co*-LA-*co*-3HV) is a terpolymer consisting of 3-hydroxybutyrate (3HB), lactic acid (LA) and 3-hydroxyvalerate (3HV). Each component contributes distinct properties to this biopolymer, making it a promising material in the field of biodegradable plastics.[16,17] Polyhydroxybutyrate (PHB) is known for its high crystallinity and biodegradability with brittleness, limiting its applications.[18] Polylactic acid (PLA), a widely used biopolymer, is also biodegradable with flexibility and biocompatibility.[19] Poly(3-hydroxybutyrate-*co*-3-hydroxyvalerate) (PHBV) improves toughness and elasticity relative to PHB.[20,21] By combining these three monomers, P(3HB-*co*-LA-*co*-3HV) achieves adjustable thermo-mechanical and biodegradation properties via monomer ratio optimization.

Previous studies have reported the synthesis of the terpolymer P(3HB-*co*-8.7 mol% LA-*co*-7.2 mol% 3HV) in a genetically engineered lactate-overproducing *Escherichia coli* JW0885 grown with propionate supplementation, where monomer ratios were modulated by adjusting propionate concentrations.[22] However, challenges remain in achieving precise compositional control, as 3HV incorporation was restricted to a narrow range (0-7.2 mol%) while elevated propionate levels (> 100 mg L^{-1}) suppressed total polymer accumulation due to substrate toxicity.[22] Additionally, scalable production of such terpolymers requires energy-intensive sterile fermentation, highlighting the need for alternative microbial platforms compatible with cost-effective industrial processes.

The halophilic bacterium *H. bluephagenesis* is considered as a chassis organism for NGIB, which has been engineered to enable cost-effective production of various polyhydroxyalkanoates (PHAs) and other high-value compounds under non-sterile and continuous fermentation conditions.[6,23] *H. bluephagenesis* is naturally capable of synthesizing PHB.[24] Engineered the bacterium allows productions of P(3-hydroxybutyrate-*co*-3-hydroxypropionate) P(3HB-*co*-3HP); P(3-hydroxybutyrate-*co*-4-hydroxybutyrate), (P34HB); P(3-hydroxybutyrate-*co*-3-hydroxyvalerate (PHBV); P(3-hydroxybutyrate-*co*-5-hydroxyvalerate, P(3HB-*co*-5HV); P(3-hydroxybutyrate-*co*-3-hydroxyhexanoate), PHBHHx. PHB, P34HB and PHBV. Typically, *H. bluephagenesis* provides feasibility of large-scale industrial production with reduced costs.[25-29] Despite these advancements, the biosynthesis of LA-containing terpolymers such as P(3HB-*co*-LA-*co*-3HV) has not yet been explored in *H. bluephagenesis*. Addressing this gap could expand the range of PHA materials while leveraging the industrial scalability.

This study focused on engineering *H. bluephagenesis* for P(3HB-*co*-LA-*co*-3HV) production with a controllable LA and 3HV ratios for flexible material properties, it was conducted following a sequential framework of "construction of engineering strain, its performance optimization, process scale-up and material characterization".

MATERIAL AND METHODS

Strains and media

The strains, plasmids, and genes employed in this study are summarized in Table 1 and Table S1. The halophilic wildtype bacterium *Halomonas bluephagenesis* TD01 was originally obtained from Aydingol Lake located in the Xinjiang region of China. *E. coli* S17-1 was used for plasmid construction and vector donation during conjugation, while *E. coli* DH5α, obtained from

Table 1. Strains and plasmids used in this study.

Strains/Plasmids	Description	Source/ literature
Strains		
Escherichia coli (*E. coli*) S17-1	Harboring the *tra* gene on the chromosome, used for conjugation	[34]
Halomonas. bluephagenesis (*H. bluephagenesis*) TD01	wild type strain, isolated from Aydingkol Lake of Xinjiang Province, China	[24]
H. bluephagenesis TD1.0	Carrying $P_{T7\text{-}like}$ RNA polymerase expression module on *H. bluephagenesis* TD01	[35]
Clostridium propionicum	Source of the pct_{540} gene	Lab stocks
Pseudomonas sp. 6-19	Source of the $phaC_{1437}$ gene	Lab stocks
CJN01	Genomic deletion of $phaC_{TD}$ gene of *H. bluephagenesis* TD1.0 derivate	This study
CJN19	Genomic insertion of $P_{porin\ RE}$- $phaC_{1437}$- pct_{540} unit in G4/GY2/G51/PhaP1 sites of *H. bluephagenesis* CJN01 derivate	This study
CJN28	Genomic deletion of *dld* and *pta* genes of *H. bluephagenesis* CJN19 derivate	This study
CJN32	Genomic deletion of *mreB* gene of *H. bluephagenesis* CJN28 derivate	This study
Plasmids		
pSEVA321	An expression vector harboring RK2 replication origin, *ori*T sequence for conjugation in *H. bluephagenesis*, Cm^R	[36]
pSEVA341	High copy number expression vector used for overexpression, pRO1600/ColE1 replication origin, *oriT*, Cm^R	[36]
pQ08	pSEVA321 derivative, expressing *S. pyogenes* cas9, Cm^R	[29]
pgR-G4	pSEVA341 derivative, G4 genomic site sgRNA with integrated expression cassette, 1000 bp donor,Km^R and Spe^R	This study
pgR-GY2	pSEVA341 derivative, GY2 genomic site sgRNA with integrated expression cassette, 1000 bp donor,Km^R and Spe^R	This study
pgR-G51	pSEVA341 derivative, G51 genomic site sgRNA with integrated expression cassette, 1000 bp donor,Km^R and Spe^R	This study
pgR-PhaP1	pSEVA341 derivative, PhaP1 genomic site sgRNA with integrated expression cassette, 1000 bp donor,Km^R and Spe^R	This study
pgR-$phaC_{TD}$	pSEVA341 derivative $phaC_{TD}$ knockout, $phaC_{TD}$ sgRNA, homologous arm length 1000 bp, Km^R and Spe^R	This study
pgR-pta	pSEVA341 derivative *pta* knockout, *pta* sgRNA, homologous arm length 1000 bp, Km^R and Spe^R	This study
pgR-dld	pSEVA341 derivative *dld* knockout, *dld* sgRNA, homologous arm length 1000 bp, Km^R and Spe^R	This study
pgR-sdhE	pSEVA341 derivative *sdhE* knockout, *sdhE* sgRNA, homologous arm length 1000 bp, Km^R and Spe^R	This study
pgR-prpC	pSEVA341 derivative *prpC* knockout, *prpC* sgRNA, homologous arm length 1000 bp, Km^R and Spe^R	This study
pgR-mreB	pSEVA341 derivative *mreB* knockout, *mreB* sgRNA, homologous arm length 1000 bp, Km^R and Spe^R	This study
pI-Hfq-Null	pSEVA321 derivative, inducible expression of *hfqEc* controlled by the external addition of IPTG, Cm^R	This study
pI-Hfq-X	pSEVA321 derivative, inducible expression of *hfqEc* controlled by the external addition of IPTG, Cm^R $fadB_{1/2/3/4/5/6/7/8}$ or $fadA_{1/2/3/4/5}$ homologous arm length 1000 bp,	This study
pI-Hfq-A	pSEVA321 derivative, inducible expression of *hfqEc* controlled by the external addition of IPTG, *phaA* homologous arm length 1000 bp, Cm^R	This study
pI-Hfq-B	pSEVA321 derivative, inducible expression of *hfqEc* controlled by the external addition of IPTG, *phaB* homologous arm length 1000 bp, Cm^R	This study
pCJN68	pSEVA321 derivative, inducible expression of *scpAB* controlled by the external addition of IPTG, Cm^R	This study

Tsingke Co. Ltd. (China), was used for general cloning purposes.

E. coli cultivation was performed in LB supplemented with 10 g L^{-1} tryptone, 5 g L^{-1} yeast extract and 10 g L^{-1} NaCl. *H. bluephagenesis* TD01 and its derivatives were cultured in LB containing 60 g L^{-1} NaCl, with the remaining components as described above. Both *E. coli* and *H. bluephagenesis* were cultured at 37°C and 200 rpm. Shake flask experiments were conducted in 50 MM. All 50 MM contain 1 g L^{-1} yeast extract, 0.5 g L^{-1} urea, 50 g L^{-1} NaCl, 0.2 g L^{-1} $MgSO_4$, 3.83 g L^{-1} Na_2HPO_4, 1.5 g L^{-1} KH_2PO_4, 0.01 mg L^{-1} trace element solution-I and 0.001 g L^{-1} trace element solution-II. Component solution I and II are same as prior methods.[30] The pH of the media was adjusted to a range of 8.0 to 9.0. To ensure the stability of the target plasmids in various recombinants *H. bluephagenesis*, 25 mg L^{-1} chloramphenicol and/or 100 mg L^{-1} spectinomycin were added.

Plasmid construction methods and genome editing tools

Plasmids were synthesized primarily using the Gibson Assembly technique.[31] PCR amplification of DNA fragments was carried out with Q5 High-Fidelity DNA Polymerase (New England Biolabs, Inc., USA), followed by purification using a gel purification kit (Omega, USA). Target gene fragments were assembled with the Gibson Assembly kit (NEB, USA). The resulting ligation products were subsequently introduced into *E. coli* S17-1 or DH5α for bulk amplification. Positive clones, identified through DNA sequencing, were then prepared for further experimentation. Genome editing in *H. bluephagenesis* was accomplished using the CRISPR/Cas9, ClpXP degradation and PrrF1-2-HfqPa systems.[28,32,33] Chemicals were sourced from Sinopharm Chemical Reagent (China) and Sigma-Aldrich (USA), while primers were synthesized by Xianghong Biotech (China). DNA sequencing was carried out by Tsingke (China).

Conjugation transformation

Plasmids were successfully introduced into *H. bluephagenesis* via conjugation. The donor strain used was *E. coli* S17-1 λpir. Both *H. bluephagenesis* and *E. coli* S17-1 λpir harboring the plasmids, were cultured for 4 hours at

37 °C to reach an OD_{600} of 0.4. Centrifugation was performed to collect 1 mL of cells from each strain. The pellets were then resuspended in LB, combined in a 1:1 ratio, and cultivated for 24 hours at 37°C on 20-LB plates. Following this, the bacterial mixture was spread onto 60 LB solid plates supplemented with the appropriate selective antibiotics and incubated for an additional 24 hours at 37°C. Individual colonies were isolated and verified by PCR.

Shake flask and fed-batch studies

A single colony of *H. bluephagenesis* TD1.0 or its derivatives was inoculated into 60 LB and cultured for 10-12 hours at 37°C in a shake flask (total volume 500 mL, working volume 50 mL). The second seed culture was obtained by transferring 200 μL of the initial culture into fresh 60 LB, followed by incubation for 8-10 hours. Subsequently, 50 mL of 60 MMG was added to 2.5 mL of seed culture in a 500 mL shake flask, and the mixture was incubated at 37°C with shaking at 200 rpm for 48 hours. *H. bluephagenesis* TD1.0 and its derivatives were cultivated in 60 LB for seed activation and growth in this study. LB contained 5 g L^{-1} yeast extract, 10 g L^{-1} tryptone and 10 g L^{-1} NaCl. For PHA accumulation, *H. bluephagenesis* TD1.0 and its derivatives were cultivated in 60 MMG during shake flask experiments. The composition of the 60 MMG included 10 mL L^{-1} trace element solution I and 1 mL L^{-1} trace element solution II, 60 g L^{-1} NaCl, 1 g L^{-1} yeast extract, 0.7 g L^{-1} $(NH_2)_2CO$, 0.2 g L^{-1} $MgSO_4$, 9.65 g L^{-1} $Na_2HPO_4{\cdot}12H_2O$, 1.5 g L^{-1} KH_2PO_4, and 30 g L^{-1} glucose. Trace element solution I contained 1 M HCl, 5 g L^{-1} Fe(III)-NH_4-citrate, and 2 g L^{-1} $CaCl_2$. Trace element solution II contained 30 mg L^{-1} $Na_2MoO_4{\cdot}2H_2O$, 20 mg L^{-1} $NiCl_2{\cdot}6H_2O$, 10 mg L^{-1} $CuSO_4{\cdot}5H_2O$, 200 mg L^{-1} $CoCl_2{\cdot}6H_2O$, 300 mg L^{-1} H_3BO_3, 30 mg L^{-1} $MnCl_2{\cdot}4H_2O$, and 100 mg L^{-1} $ZnSO_4{\cdot}7H_2O$. The pH of the medium was adjusted to approximately 8.0-8.5 using 5 M NaOH.

Analysis of cell dry weights and their P(3HB-*co*-LA-*co*-3HV) contents

The cell dry weight (CDW) was quantified by lyophilizing the cell pellets obtained from 50 mL of fermentation broth: after centrifugation at 9,600 × g for 30 min (CR 21GIII, HITACHI, Japan), the pellets were washed with distilled water and subjected to a lyophilization process at -80°C for 0.5-1 h followed by vacuum drying for 16-24 h. For the esterification reaction, 30 to 40 mg of the lyophilized cells were finely ground into powder and heated in a 15 mL tube at 100°C for 4 hours, in the presence of 4 mL of esterification mixture containing 2 mL of methanolysis solution (85 wt% methanol, 15 wt% H_2SO_4, 1 g L^{-1} benzoic acid) and 2 mL of chloroform. Both the content and monomeric composition of the synthesized polyhydroxyalkanoate (PHA) were determined via gas chromatography analysis using a SHIMADZU GC-2014 system. Standards of 10-30 mg P(3HB) (99.9%, Sigma-Aldrich), lactic acid (99%, Sigma-Aldrich) and 3-hydroxyvalerate (3HV unit standard; Sigma-Aldrich, USA) were used.

Microscopy

Sample preparation for transmission electron microscopy (TEM) involved a series of procedures: cells were harvested from shake flasks by centrifugation at 1,500 × g for 3 min, washed once with PBS (pH 7.2), and finally fixed with 2% glutaraldehyde (pH 7.2) at 4°C for 4 hours.

Following the fixation, the cells were subsequently stained employing a solution of 0.05% ruthenium red in 0.1 M cacodylate buffer at 4°C for a duration of 5 hours. After being washed with the same buffer, the cells were subjected to post-fixation in 1% osmium tetroxide supplemented with 0.05% ruthenium red at 4°C for 2 h. Subsequently, the samples were rinsed again with cacodylate buffer and processed through a graded ethanol series for dehydration. The dehydrated specimens were then embedded in resin and sectioned into 80 nm slices using an ultra-microtome (Leica, Germany). Finally, the sections were examined with a TEM system (H-7650B, Japan) operating at an accelerating voltage of 80 kV.

PHA extraction and purification

Intracellular PHA was isolated from the lyophilized cell biomass by employing a Soxhlet extraction system (Soxtec 2050, Foss, Denmark) via the established procedure: the dried cells were treated by boiling at 110°C for 3 hours, eluting for 2 hours, and finally recycling for 1 hour. PHA polymers were purified by redissolving the extracted samples in chloroform and precipitating with an 8-fold volume of ethanol.

Gel permeation chromatography (GPC)

GPC was performed on an LC-20AD system (SHIMADZU, Japan) to assess the molar mass and polydispersity of the samples, using a SHIMADZU GPC-804C column fitted with a refractive index detector (SHIMADZU, Japan). The samples were dissolved in chromatographically pure chloroform at a concentration of 2 mg mL^{-1}. Any remaining substance was filtered using a 0.22 μm nylon-membrane syringe filter (Jinglong, China). Chromatographically pure chloroform was used as the mobile phase, with an injection volume of 40 μL and a flow rate of 1 mL min^{-1} at 40°C. A series of number-average molar masses of polystyrene standards (1×10^4, 2×10^4, 3×10^4, 7×10^4, 1.5×10^5, 3×10^5, 7×10^5 and 1×10^6, Sigma-Aldrich, USA) were employed to calibrate the system.

Differential scanning calorimetry (DSC)

A DSC-Q20 device (TA, USA) was used to obtain polymer differential scanning calorimetry (DSC) data. Nitrogen was used as the purge gas, with a flow rate of 50 mL min^{-1}. The temperature range was set from -80°C to 200°C. Samples were first cooled to -80°C and then heated at a rate of 10°C min^{-1} from -80°C to 180°C. For the second cycle, the samples were reheated and quenched again within the same temperature range.

Thermal gravimetry analysis (TGA)

The thermal stability of the PHA samples was evaluated using a TGA-50 analyzer (Shimadzu, Japan). Approximately 5-10 mg of each sample was subjected to a controlled temperature ramp from ambient temperature to 600°C at a heating rate of 10°C min^{-1} under a continuous nitrogen purge.

Mechanical property studies

PHA films were cast by dissolving 1 g of the purified sample in 15-20 mL of chloroform on glass disks with a diameter of 60 mm. The films were carefully cut into dumbbell-shaped samples (width: 4 mm) using an RR/PCP machine (Ray-Ran, UK). Stress-strain measurements were conducted using an Instron 3365 tensile-strength measurement device (Instron, USA) with a stretching speed of 10 mm min^{-1}. Each sample was tested in triplicate, and the average values were reported.

RESULTS

De novo biosynthesis of P(3HB-*co*-LA-*co*-3HV) by *H. bluephagenesis*

The wild-type *H. bluephagenesis* synthesizes PHB. The engineered strain *H. bluephagenesis* CJN28 integrates four copies of codon-optimized pct_{540*} (propionyl-CoA transferase) and $phaC_{1437}$ (LA-associated synthase) into its genome, with deletion of *pta* and *dld* genes encoding phosphate acetyltransferase and D-lactate dehydrogenase, respectively (Figure 1A). This engineered strain successfully produced P(3HB-*co*-LA) using glucose as the sole carbon source. Previous studies have demonstrated that 3HV biosynthesis can be achieved by propionate supplementation during glucose fermentation, although this method inhibits cellular growth and increases production costs.[37] Redirecting metabolic flux toward 3HV synthesis offers a cost-effective approach while maintaining normal cell growth.[38] Deletion of the *sdhE* (encoding succinate dehydrogenase assembly factor 2) and *prpC* (encoding 2-methylcitrate synthase), enhances propionyl-CoA utilization for 3HV production (Figure 1A).[25] The heterologous expression module *scpAB* operon encoding methylmalonyl-CoA mutase and methylmalonyl-CoA decarboxylase,[25] was employed to redirect TCA cycle intermediates to 3HV component synthesis (Figure 1A). *H. bluephagenesis* CJN28△*sdhE*△*prpC* harboring pSEVA321-*mmp1-scpAB* was induced with different IPTG concentrations (Figures 1B & C). The 3HV content showed a bell-shaped response to increasing IPTG concentrations. Optimal 3HV production occurred at 2 mg L^{-1} IPTG (Figure 1C). This induction condition reached 7.45 g L^{-1} CDW containing 51% P(3HB-*co*-LA-*co*-3HV), with the 3HV content remained below 1 mol% under glucose-based cultivation (Figure 1C). While the first successful *de novo* synthesis of P(3HB-*co*-LA-*co*-3HV) from glucose was achieved, the low conversion efficiency motivated subsequent experimental implementation of precursor supplementation strategies to optimize terpolymer biosynthesis.

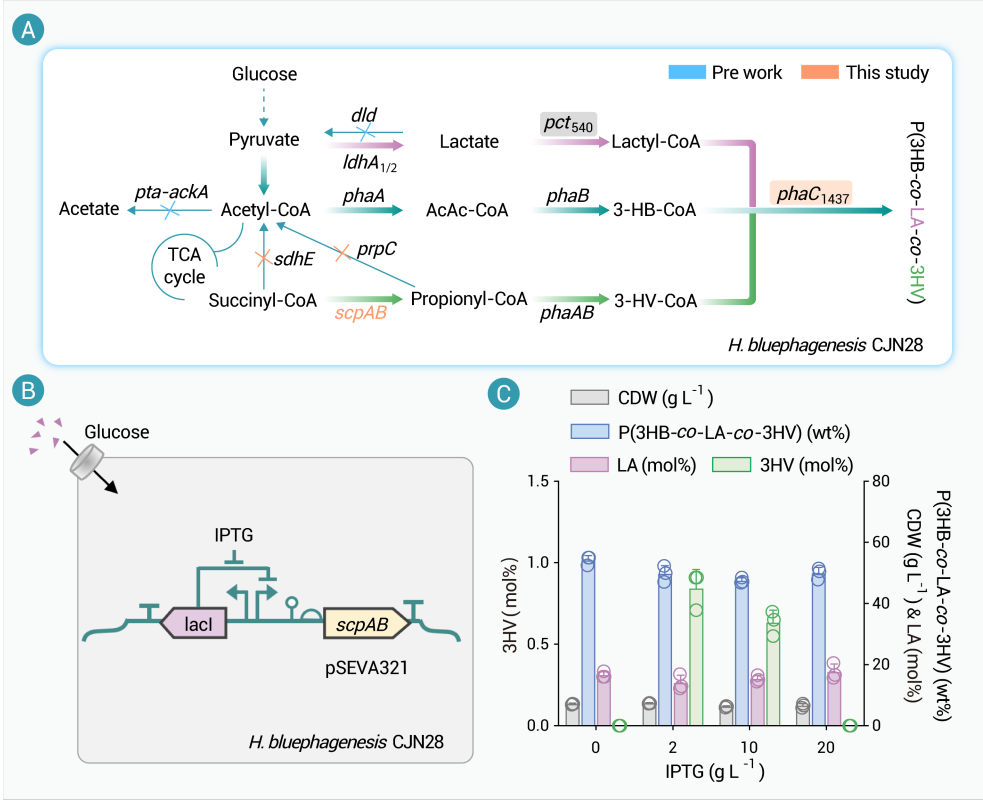

Figure 1. ***De novo*** **production of P(3HB-*co*-LA-*co*-3HV) by *H. bluephagenesis* CJN28△*sdhE*△*prpC* harboring pSEVA321-*mmp1-scpAB* grown on glucose** (A) Metabolic engineering of *H. bluephagenesis* for *de novo* synthesis of P(3HB-*co*-LA-*co*-3HV from Glucose. SdhE, succinate dehydrogenase. PrpC, 2-methylcitrate synthase. (B-C) Production of P(3HB-*co*-LA-*co*-3HV) by *H. bluephagenesis* CJN28△*sdhE*△*prpC* harboring pSEVA321-*mmp1-scpAB* in the presence of mmp1 inducible system induced using different concentrations of IPTG.

P(3HB-*co*-LA-*co*-3HV) synthesis by *H. bluephagenesis* grown on glucose and sodium valerate

The wild-type *H. bluephagenesis* synthesized PHBV in 50 MM medium containing sodium valerate.[30] Sodium valerate tolerance was evaluated by culturing *H. bluephagenesis* in 96-well plates with 0, 10, 30 and 50 g L^{-1} sodium valerate for 48 h. It was found that *H. bluephagenesis* showed significant tolerance to sodium valerate (Figure S1), demonstrating potential for 3HV-containing PHA biosynthesis using sodium valerate as a substrate. For P(3HB-*co*-LA-*co*-3HV) production, engineered strains were cultured in 50 MM medium with 10 g L^{-1} sodium valerate. Excitingly, *H. bluephagenesis* CJN28 was able to synthesize 1.20 g L^{-1} CDW with 33.90 wt% P(3HB-*co*-9.18 mol% LA-*co*-2.88 mol %3HV) (Figure 2). GC and ^{1}H NMR analyses verified the chemical structure (Figure S1). Specifically, the ^{1}H NMR spectrum unambiguously confirmed the simultaneous incorporation of three monomeric units: 3HB, 3HV, and LA. All characteristic proton signals of the three units were distinctly observed and assigned, as labelled in Figure S1. The clear assignment of all expected signals, with no extraneous peaks indicative of impurities or homopolymer blends, provides direct spectroscopic evidence that the product is a chemically well-defined terpolymer, rather than a physical mixture.However, both PHA content and biomass production remain suboptimal. Subsequent process optimization will focus on enhancing terpolymer biosynthesis efficiency.

The effects of sodium valerate concentration, supplementation timing, and glucose-to-salt ratios on P(3HB-*co*-LA-*co*-3HV) production were systematically evaluated (Figure S2). Initial sodium valerate supplementation (1-5 g L^{-1}) in 50 MM medium enhanced terpolymer biosynthesis. *H. bluephagenesis* CJN28 achieved maximum production of 5.14 g L^{-1} P(3HB-*co*-LA-*co*-3HV) (83.49 wt%; 12.55 mol% LA, 67.76 mol% 3HV) with 5 g L^{-1} sodium valerate in 50 MM medium, reaching 6.16 g L^{-1} CDW (Figure S2A).

Time-course optimization revealed peak terpolymer yield (6.42 g L^{-1}) when supplementing 5 g L^{-1} sodium valerate at 24 h in 50 MM medium, producing 71.54 wt% P(3HB-*co*-LA-*co*-3HV) (16.90 mol% LA, 34.65 mol% 3HV) with 8.97 g L^{-1} CDW (Figure S2B). Subsequent glucose/salt ratio optimization (30 g L^{-1} glucose, 50 g L^{-1} salt) in sodium valerate-supplemented 50 MMV medium at 24 h increased production to 9.48 g L^{-1} (Figure 2C). The optimized 50 MMV formulation was therefore selected (Figures S2D-G).

The buffer solution in the culture medium was used to maintain a stable pH, ensuring optimal growth conditions for *H. bluephagenesis*. The addition of varying concentrations of the MOPS buffer to the culture medium revealed that *H. bluephagenesis* CJN28 synthesized P(3HB-*co*-LA-*co*-3HV) with significantly reduced 3HV content (Figure S2). While prior studies showed yeast extract (1→3 g L^{-1}) enhanced P(3HB-*co*-LA) production, this adjustment failed to improve P(3HB-*co*-LA-*co*-3HV) content (Figure S2). Therefore, the optimal medium for synthesizing P(3HB-*co*-LA-*co*-3HV) in this study was determined to be 50 MMV containing glucose and salt concentrations of 30 g L^{-1} and 50 g L^{-1}, respectively, supplemented with 5 g L^{-1} sodium valerate at 24 hours. However, yeast extract and buffer were found to have no significant effect on the production yield of this novel terpolymer.

Enhanced 3HV and LA ratio in P(3HB-*co*-LA-*co*-3HV) by *β*-oxidation weakened *H. bluephagenesis*

The 3HV component of P(3HB-*co*-LA-*co*-3HV) is synthesized via the fatty acid *β*-oxidation pathway when sodium valerate is utilized as the carbon source. This process produces trans-2-enoyl-CoA, which is subsequently converted by the PhaJ enzyme into (R)-3-hydroxyvaleryl-CoA. It ultimately results in the formation of 3HV in P(3HB-*co*-LA-*co*-3HV) (Figure 2A). Additionally, each cycle of *β*-oxidation generates acetyl-CoA, which is utilized to form both the 3HB and LA components in P(3HB-*co*-LA-*co*-3HV) (Figure 2A). Therefore, to further improve the 3HV ratio, the *β*-oxidation cycle should be attenuated. The critical functional proteins in the *β*-oxidation pathway of *H. bluephagenesis* include enoyl-CoA hydratase and 3-ketoacyl-CoA thiolase encoded by *fadB* and *fadA* genes, respectively. Based on the genomic annotation of *H. bluephagenesis* TD01, multiple candidate *fadB* genes and *fadA* genes were identified.[29]

In order to examine the changes in the expression levels of the *fadB* and *fadA* genes upon sodium valerate addition, both the control group and the sodium valerate-treated one were cultured in shake flasks containing 50 MM for 48 hours, after which RNA-seq analysis was conducted to assess the effects of sodium valerate. The log2 transcript ratio of the sodium valerate-treated group (T) to the control group (D) was utilized to select genes, with significance set at $P < 0.05$ and $|\log2\ \text{ratio}| > 1$. Consequently, 531 genes were downregulated, and 373 genes were upregulated in *H. bluephagenesis* CJN28 (Figures 3A & B). Unexpectedly, no significantly differential genes were detected in the *β*-oxidation pathway, potentially due to their constitutive genomic expression. Therefore, comparative analysis of expression differences was conducted for 11 candidate genes annotated in the genome, followed by experimental validation (Figure 3C).

The PrrF1-2-HfqPa system is a new synthetic sRNA system that is based on PrrF1 scaffold and HfqPa from *P. aeruginosa* for controlling gene expression.[33] In this study, the candidate genes were deleted using the PrrF1-2-HfqPa system (Figures 3D-F & Table S2). *H. bluephagenesis* CJN28, harboring the plasmid of the PrrF1-2-HfqPa system with targeted binding to $fadB_n$ and $fadA_n$, was cultured in 50 MMV for 48 h.The shake flask results showed that both the *fadB* and *fadA* group, which showed decreased expression levels, resulted in a significant increase in either the 3HV or LA component (Figure 3G). The knockdown efficiency of each gene is provided in Figure S4, and RT-PCR results confirmed that their expression was significantly

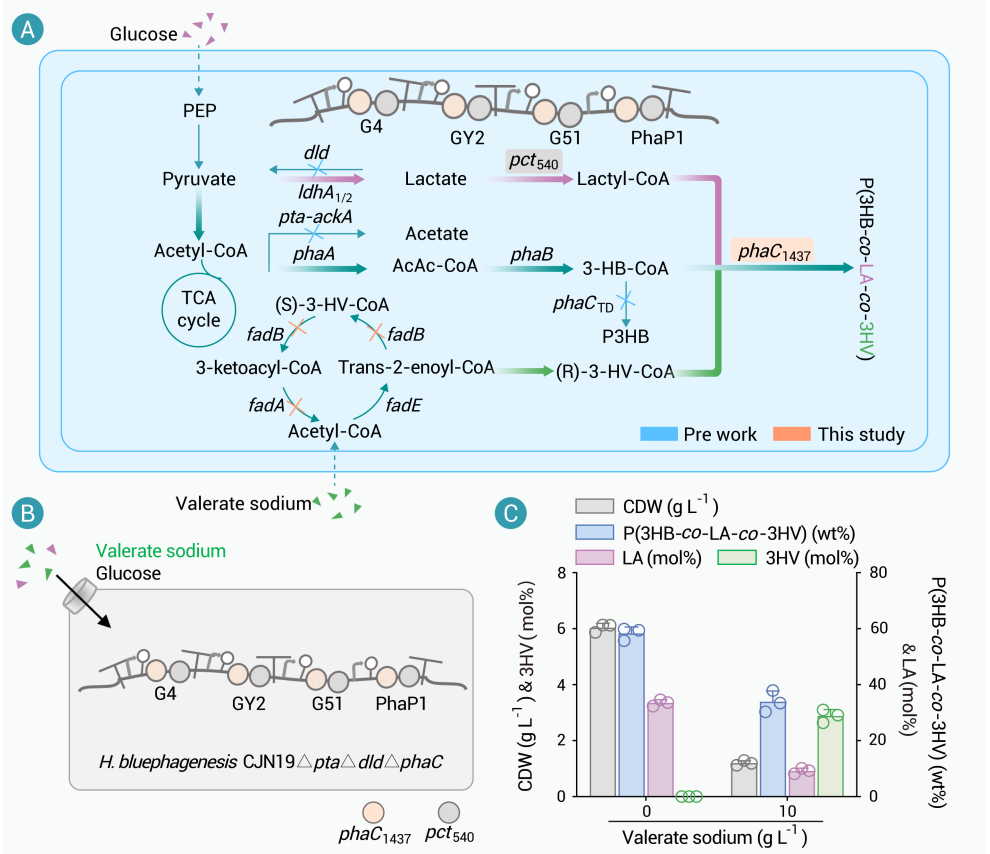

Figure 2. P(3HB-*co*-LA-*co*-3HV) synthesis by engineered *H. bluephagenesis* grown on glucose and sodium valerate (A) Poly(3-hydroxybutyrate-*co*-lactate-*co*-3-hydroxyvalerate), abbreviated as P(3HB-*co*-LA-*co*-3HV), was synthesized by *H. bluephagenesis* using glucose and sodium valerate as substrates. Glucose served as the substrate for generating 3HB-CoA and lactyl-CoA, where 3HB-CoA is obtained from the PhaA and PhaB forming 3HB monomers, with lactyl-CoA converted into LA monomers via the $LdhA_{1/2}$ and Pct_{540}. Concurrently, sodium valerate was metabolized into 3HV-CoA via either the native or weakened *β*-oxidation pathway, ultimately contributing to the biosynthesis of the P(3HB-*co*-LA-*co*-3HV) terpolymer by *H. bluephagenesis*. FadL, fatty acid transport; FadE, acyl-CoA dehydrogenase; FadB, enoyl-CoA hydratase; FadA, 3-ketoacyl-CoA thiolase; $PhaJ_{TD}$, native enoyl-CoA-hydratase; PhaA, 3-ketothiolase; PhaB, acetoacetyl-CoA reductase; $PhaC_{1437}$, PHA synthase (*Pseudomonas sp.*); $PhaC_{TD}$, native PHA synthase; $LdhA_{1/2}$, native lactate dehydrogenase; Pct_{540}: propionyl-CoA transferase. (B) The *H. bluephagenesis* TD1.0△*phaC* genome was engineered by integrating 4 copies of the pct_{540}-$phaC_{1437}$ operon and deleting PLA-competing pathway genes (*pta* and *dld*), resulting in the engineered *H. bluephagenesis* CJN28, which produced P(3HB-*co*-LA-*co*-3HV) using glucose and sodium valerate as carbon substrates. Pta: phosphate acetyltransferase; Dld, lactate dehydrogenase. (C) Comparison of production of P(3HB-*co*-LA-co-3HV) by *H. bluephagenesis* CJN28 in a 50 MM including 30 g L^{-1} glucose with 0 or 10 g L^{-1} sodium valerate as carbon sources.

reduced. For instance, the knockdown of $fadB_1$ significantly increased the 3HV ratio from 5 mol% to 58 mol%, together with an increased PHA content. The knockdown of $fadB_4$ significantly enhanced the LA ratio from 18 mol% to 48 mol% (Figure 3G). As a preliminary mechanistic explanation: FadB1 likely prefers medium-chain acyl-CoA substrates (C4-C6), and its knockdown preferentially increased 3HV synthesis; FadB4 may participate in feedback regulation or branch-point control of *β*-oxidation, and its knockdown redirects upstream intermediates toward LA synthesis. The *phaA* and *phaB* genes, involved in the PHB synthesis pathway, were inhibited by this system, resulting in a 3HV ratio from 5 mol%, 55 mol% and 43 mol%, respectively (Figure S3). Unfortunately, this system also resulted in inhibited bacterial growth and a reduction in PHA accumulation. The observed decrease in cell growth in terms of CDW is attributed to two main factors: the metabolic burden imposed by the exogenous plasmid-based PrrF1-2-HfqPa system and the growth impairment resulting from extensive genomic modifications, including the knockout of endogenous *phaC* and integration of heterologous genes. These combined effects explain the significantly lower biomass compared to the control *H. bluephagenesis* strain producing PHB.

Enhanced P(3HB-*co*-LA-*co*-3HV) synthesis by morphologically engineered *H. bluephagenesis*

Genetic manipulations that influence bacterial morphology can result in the formation of fibers or larger spherical structures.[12,39] Enlarged bacterial cells accelerate cell growth (CDW), simplify downstream separation and promote greater accumulation of inclusion bodies.[39,40] The *mreB* gene encodes an actin-like cytoskeleton that plays a key role in determining the rod shape of bacterial cells.[41,42] Earlier study has shown that deleting the *mreB* gene converts cells from a rod-like morphology to a spherical shape.[12] Based on *H. bluephagenesis* CJN28, the *mreB* gene was modulated via the ClpXP degradation system by deleting *sspB* and using mutated SsrA12 tag with slow degradation rate,[28] named as *H. bluephagenesis* CJN32 (Figure 4A). This strategy allows precise control of MreB degradation for functional analysis.[28]

To examine the growth and P(3HB-*co*-LA-*co*-3HV) synthesis of cytoskeleton-defective *H. bluephagenesis*, shake flask studies were performed in a 50 MMV. This medium supported growth to 10.75 g L^{-1} CDW containing 85.78 wt% P(3HB-*co*-14.60 mol% LA-*co*-39.82 mol% 3HV) in *H. bluephagenesis* CJN32 (Figure 4B). Compared to *H. bluephagenesis* CJN28, CDW and P(3HB-*co*-LA-*co*-3HV) production increased by 10% and 15%, respectively (Figure 4B). Transmission electron microscopy (TEM) at 1,000× magnification showed that *H. bluephagenesis* CJN32 developed a spherical morphology with a marked increase in cell volume compared to *H. bluephagenesis* CJN28 following a 48 h of shake flask growth (Figures 4C & D). Previous studies have indicated that larger cells facilitate precipitation.[43] Consequently, *H. bluephagenesis* CJN32 could improve the efficiency of downstream processing, thereby reducing both time and cost.

P(3HB-*co*-LA-*co*-3HV) production by *H. bluephagenesis* in 7-liter bioreactors

P(3HB-*co*-LA-*co*-3HV) was produced in a 7-liter fermenter incubated with *H. bluephagenesis* CJN28 and CJN32 under open, unsterile conditions using glucose and varying concentrations of sodium valerate, respectively (Figure 5A). Sodium valerate was added at 8h of incubation, with concentrations manually maintained at 3 g L^{-1} (Low), 5 g L^{-1} (Middle), and 10 g L^{-1} (High) (Figure 5A). *H. bluephagenesis* CJN28 was grown to 75.92 g L^{-1} CDW containing 69.78 wt% P(3HB-*co*-15.92 mol% LA-*co*-4.42 mol% 3HV) under the condition of Low (L) concentrations of sodium valerate (Figures 5B-E). As the sodium valerate concentration in the medium increased, cell growth was inhibited, leading to a decrease in CDW. However, both PHA content and 3HV ratio were enhanced. *H. bluephagenesis* CJN28 was grown to a CDW of 61.65 g L^{-1}, containing 85.64 wt% P(3HB-*co*-22.51 mol% LA-*co*-25.34 mol% 3HV), under High (H) condition (Figure 6). Under Middle (M) condition, the LA ratio reached 40 mol%, which may account for the slightly lower CDW observed compared to that under H conditions (Figures 5B & E).

Under the same conditions, the *mreB*-deleted *H. bluephagenesis* CJN32 was able to more efficiently utilize sodium valerate for growth, resulting in an increase in CDW (Figures 5B & 6A). However, compared with *H. bluephagenesis* CJN28, the PHA content was lower (Figures 5C & 6B). Under H conditions, *H. bluephagenesis* CJN32 (CJN28△*mreB*) reached 65.67 g L^{-1} CDW containing 47.61 wt% P(3HB-*co*-1.14 mol% LA-*co*-33.42 mol% 3HV) (Figure 6). Simultaneously, the ratio of LA in the material decreased significantly. Consequently, the medium will be optimized to adjust the component proportions in *H. bluephagenesis* CJN32 (CJN28△*mreB*).

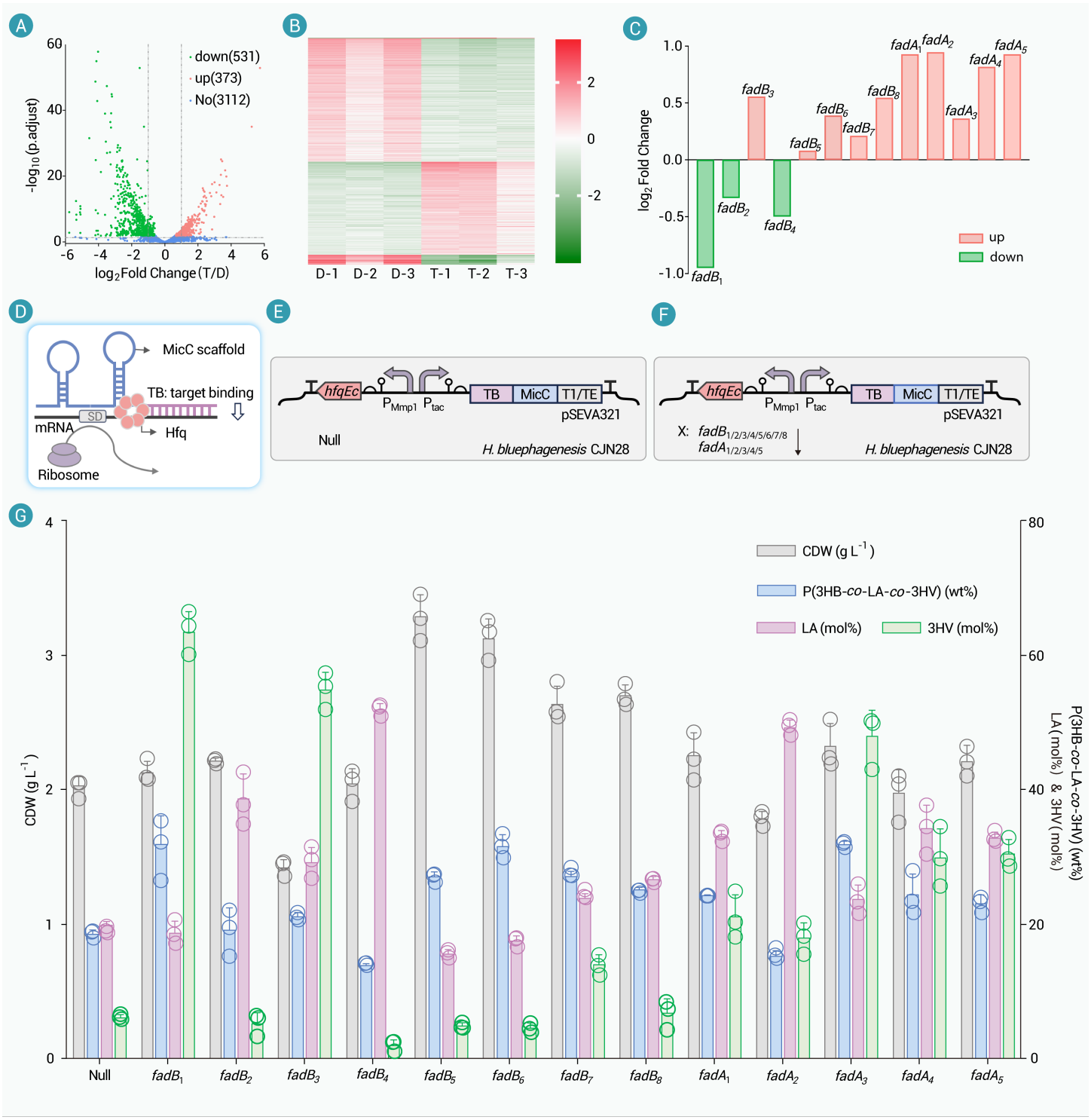

Figure 3. Differentially regulated gene expressions related to the *β*-oxidation cycle in *H. bluephagenesis* CJN28 to produce P(3HB-*co*-LA-*co*-3HV) cultured with glucose and sodium valerate (A) Volcano plot of RNA-seq (log_2 transcript ratio of *H. bluephagenesis* CJN28 grown with sodium valerate (D) or without (T). (B) Heatmap depicting differential gene expression between D and T groups in the *H. bluephagenesis* CJN28. (C) 11 genes encoding fatty acid metabolism are up- and down-regulated in *H. bluephagenesis* CJN28. (D-F) Molecular mechanism and plasmids of the PrrF1-based sRNA system underlying sRNA-mediated translational repression. (G) Biomass and content of P(3HB-*co*-LA-*co*-3HV) by *H. bulephagenesis* CJN28 deleted with *fadB*$_1$, *fadB*$_2$, *fadB*$_3$, *fadB*$_4$, *fadB*$_5$, *fadB*$_6$, *fadA*$_1$, *fadA*$_2$, *fadA*$_3$, *fadA*$_4$ and *fadA*$_5$, respectively.

These fermenter results establish *H. bluephagenesis* CJN28 as a promising platform for P(3HB-*co*-LA-*co*-3HV) production, with different proportions of the polymer components achievable by adjusting the sodium valerate concentration in the medium. *H. bluephagenesis* CJN32 (CJN28△*mreB*) with its large cell sizes shows significant potential to optimize downstream processing of P(3HB-*co*-LA-*co*-3HV).

Characterization of the material properties of P(3HB-*co*-LA-*co*-3HV) with varying compositions produced by engineered *H. bluephagenesis*

Films of P(3HB-*co*-LA-*co*-3HV) with varying monomer compositions were prepared for analysis (Figure 7A). Differential scanning calorimetry (DSC) analysis indicated a trend of decreasing melting temperature (T_m) and glass transition temperature (T_g) as the 3HV ratio increased (Figures 7B & C). In terms of elongation at break, PHB and PLA exhibited values of 6.24% and 3.76%, respectively, with PLA demonstrating lower ductility. For the terpolymer P(3HB-*co*-22.51 mol% LA-*co*-25.34 mol% 3HV), the elongation at break reached a remarkably high of 21.56%, significantly surpassing both PHB and PLA (Table S2). This improvement indicates that the incorporation of 3HV

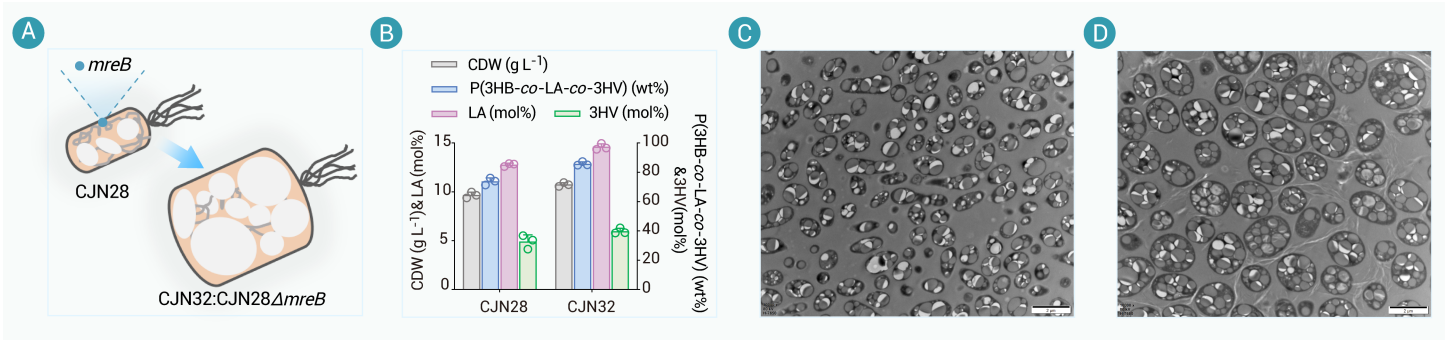

Figure 4. Engineered *H. bluephagenesis* CJN32 with enlarged cellular sizes for enhanced P(3HB-*co*-LA-*co*-3HV) production (A) The engineered *H. bluephagenesis* CJN32 was constructed by targeted deletion of the *mreB* gene in *H. bluephagenesis* CJN28. (B) Cell growth and P(3HB-*co*-LA-*co*-3HV) production by *H. bluephagenesis* CJN32 and CJN28 in 50 MM. (C-D) A comparative TEM analysis (10,000×) was performed to investigate intracellular PHA-containing *H. bluephagenesis* CJN28 and CJN32 cultured in 50 MM, respectively.

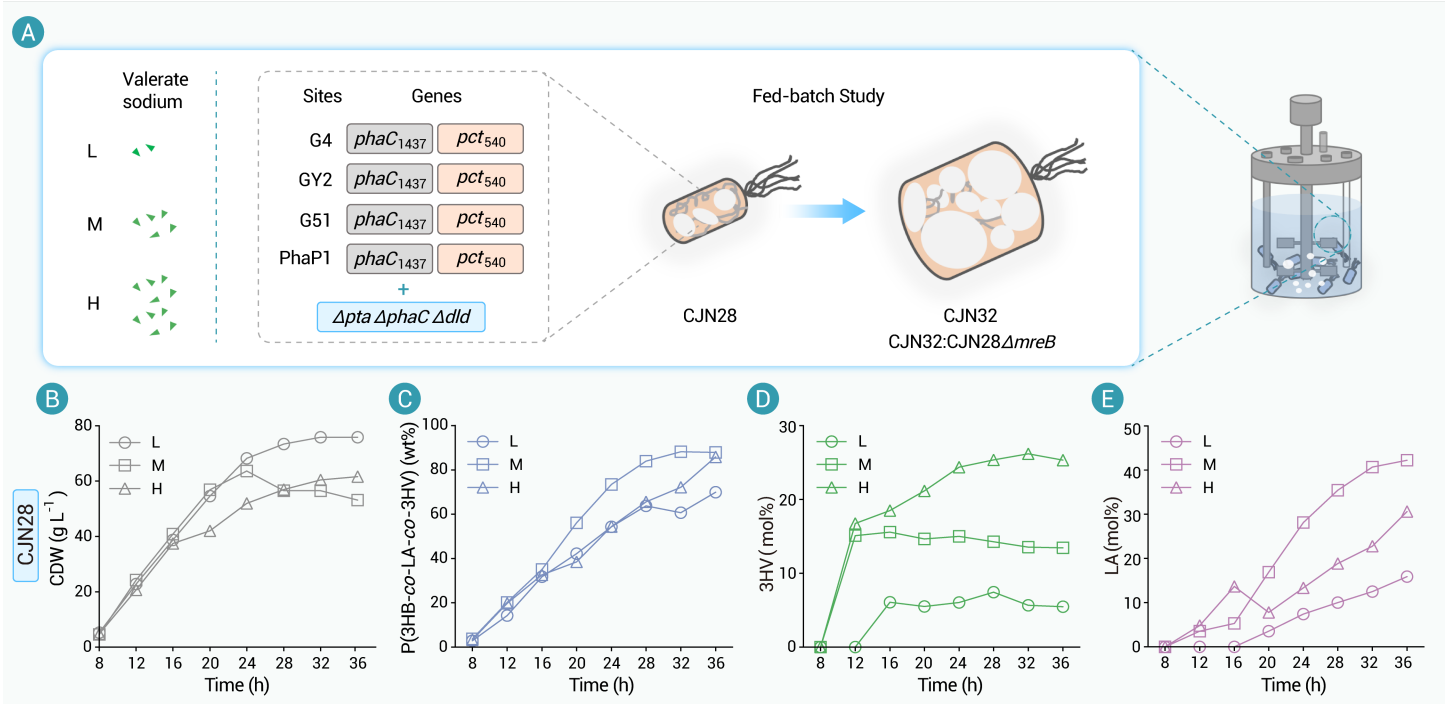

Figure 5. P(3HB-*co*-LA-*co*-3HV) production by *H. bluephagenesis* CJN28 grown in bioreactors, respectively (A) Fed-batch growth for P(3HB-*co*-LA-*co*-3HV) production by *H. bluephagenesis* CJN28 and CJN32 on glucose and different concentrations of sodium valerate as carbon sources, respectively. (B) CDW (grey), (C) P(3HB-*co*-LA-*co*-3HV) content (blue), (D) 3HV molar ratio (green) and (E) LA molar ratio (pink).

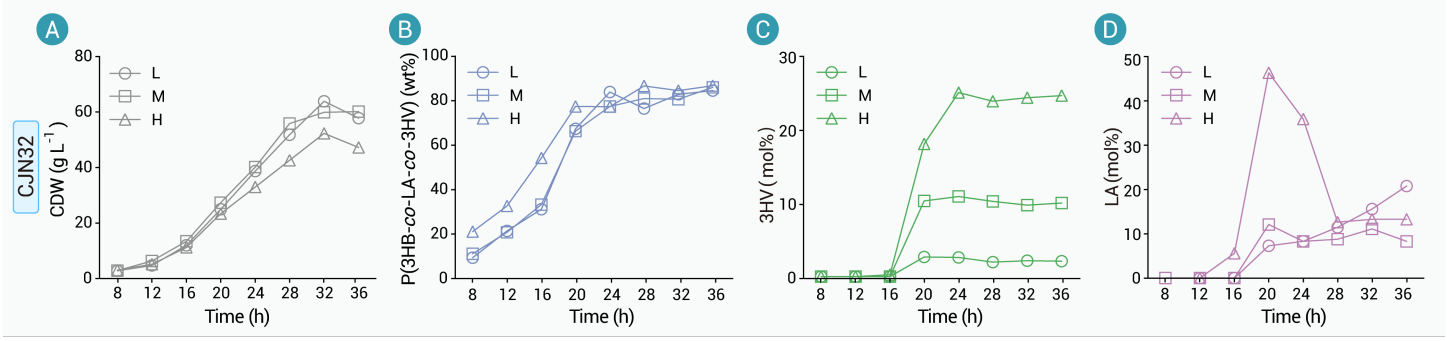

Figure 6. P(3HB-*co*-LA-*co*-3HV) production by *H. bluephagenesis* CJN32 grown in bioreactors, respectively (A) CDW (grey), (B) P(3HB-*co*-LA-*co*-3HV) content (blue), (C) 3HV molar ratio(green) and (D) LA molar ratio (pink).

substantially enhances the material toughness and ductility.

CONCLUSIONS AND DISCUSSION

Metabolically engineered *Halomonas bluephagenesis* was developed for efficient synthesis of P(3HB-*co*-LA-*co*-3HV) from glucose. Another strategy, sodium valerate supplementation enabled precise monomer tuning (0-60 mol% 3HV, 0-40 mol% LA) by knockdown of 11 β-oxidation genes or *phaA*, *phaB* enabled controllable terpolymer composition. In a 7-L bioreactor, *H. bluephagenesis* CJN28 achieved 61.65 g L^{-1} CDW with 85.64 wt% P(3HB-*co*-22.51 mol% LA-*co*-25.34 mol% 3HV) for the first time. Both CJN28 and its

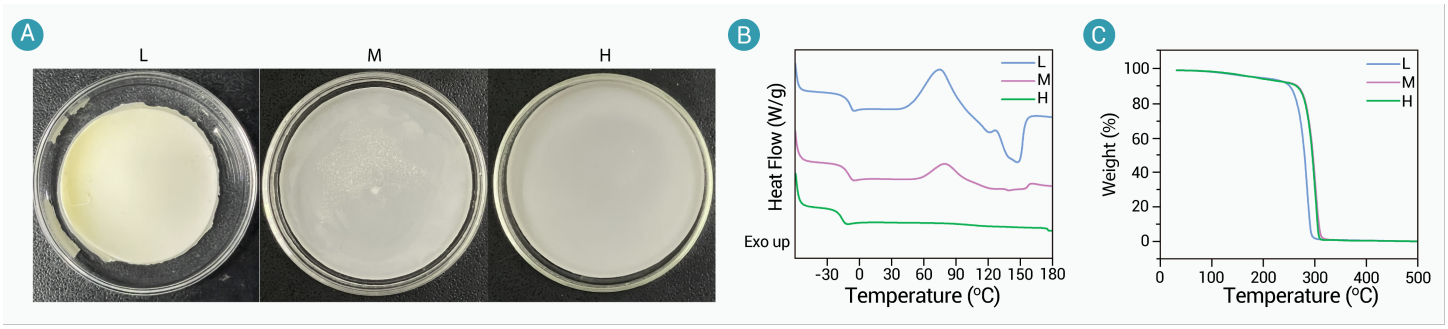

Figure 7. Thermal and mechanical properties of P(3HB-*co*-LA-*co*-3HV) consisting of different LA and 3HV ratios, respectively (A) The above PHA films. (B) DSC thermograms. (C) TGA curves. Samples: PHA terpolymers with different LA and 3HV ratios.

MreB-knockout (exhibiting enlarged cells) showed reduced downstream extraction process. The terpolymer demonstrated superior ductility over P3HB and PLA, highlighting its potential for scalable production of high-performance biopolymers.

Furthermore, the outlook for this study includes several key aspects that require further investigation and improvement. Firstly, The RNA-seq data identifies 531 downregulated and 373 upregulated genes in sodium valerate-treated cells, and systematic GO and KEGG pathway enrichment analyses for all differentially expressed genes have been conducted (see Figures S5 & S6). The core finding, as discussed, is the significant alteration in ribosome/translation processes, while the statistical support for the enrichment of fatty acid metabolism pathways was limited. This preliminary analysis indicates that classical *β*-oxidation pathways are not transcriptionally prominent under the tested conditions.

Secondly, the observed reduction in CDW (approximately 2 g L^{-1}) and PHA production during sRNA-mediated inhibition of the *β*-oxidation pathway is attributed to two primary factors. First, the introduction of the exogenous plasmid system, e.g., the constructed PrrF1-2-HfqPa system, imposes a metabolic burden on the host strain. Second, extensive genomic modifications in *H. bluephagenesis* CJN28—including knockout of the endogenous *phaC*, integration of $phaC_{1437}$-pcT_{540} of four copies, and deletion of key genes such as *pta* and *dld*—collectively impair cellular fitness. The combined effects of these factors ultimately led to the significant decrease in CDW and PHA yield in the engineered strain.

Thirdly, this study further compares the cost feasibility between glucose-only production and glucose-plus-sodium-valerate feeding. Based on current substrate prices (glucose ≈ 3,500 RMB ton^{-1}; sodium valerate ≈ 65,790 RMB ton^{-1}), the raw material cost of a basal medium containing 30 g L^{-1} glucose is about 0.105 RMB L^{-1}; adding 5 g L^{-1} sodium valerate increases the cost to 0.434 RMB L^{-1}, a rise of 313%. Therefore, when a high 3HV proportion is not required, glucose alone is preferred for low-cost screening. Sodium valerate supplementation is justified only when a specific 3HV ratio is needed for critical material properties. Ultimately, the fundamental solution to balance cost and performance lies in metabolic engineering of strains to produce high-3HV polymers from glucose alone.

Finally, P(3HB-*co*-LA-*co*-3HV) terpolymer materials exhibit unique properties. Given that monomer composition and molecular weight are key determinants of material performance, the following discussion focuses on the overall material properties and the influence of molecular weight on its applications.

Building on these findings, this study provides a comprehensive discussion on the combined effect of monomer composition and molecular weight on the material properties. The properties of P(3HB-*co*-LA-*co*-3HV) can be systematically tuned by jointly varying the LA and 3HV ratios. At low LA/3HV contents [L: P(3HB-*co*-15.92 mol% LA-*co*-4.42 mol% 3HV)], the terpolymer retains high crystallinity (T_m ≈ 150 °C), showing high modulus (~391 MPa) but extreme brittleness (elongation at break < 1%). When the LA/3HV content was increased [H: P(3HB-*co*-22.51 mol% LA-*co*-25.34 mol% 3HV)], the melting peak disappears completely, and T_g drops to about -6 °C, indicating significantly enhanced chain mobility with disappearance of crystallinity. Correspondingly, the modulus decreases (~177 MPa) while the elongation at break rose above 20%, achieving a transition from brittle to ductile behavior (Figure 6). These changes demonstrate that the incorporation of LA and 3HV disrupts the regular packing of PHB chains, promotes amorphous region formation, and thereby significantly improves toughness and processability while moderately reducing thermal stability. This provides a clear basis for tailoring material performance through monomer composition design.

The relatively low molecular weight of the terpolymers P(3HB-*co*-LA-*co*-3HV) leads to insufficient chain entanglement, resulting in brittleness and low tensile strength and modulus. For example, the σt of samples L and H is only 1.92 MPa and 8.84 MPa, respectively (Table S2). However, the comonomer composition plays a key regulatory role. Despite having the lowest molecular weight (Mn = 59,803 Da), sample M contains 42.22 mol% of LA monomer, which significantly alters its crystallization behavior. This enables it to achieve a high tensile modulus (1,659.94 MPa) and relatively high strength (11.21 MPa), although its elongation at break remains low (3.37%), indicating limited elasticity (Table S2). The mechanical properties of such low-molecular-weight terpolymers result from a combination of insufficient chain entanglement and the specific effects of comonomer composition, such as modified crystallinity and intermolecular interactions. While a low molecular weight generally impairs strength and toughness, precise regulation of copolymer ratios can still optimize certain properties, especially stiffness. Therefore, in the study of bio-based material properties, both molecular weight and the molar ratio of the constituent monomers are critical regulatory factors.

The low molecular weight of P(3HB-*co*-LA-*co*-3HV) offers distinct application advantages. This study aims to utilize this terpolymer for microsphere preparation targeting medical and cosmetic applications, as its molecular weight range is particularly suitable for microsphere formation and controlled release. In conclusion, terpolymer P(3HB-*co*-LA-*co*-3HV) provide more flexibility on material properties for medical and additive applications.

Continued efforts are still needed to elucidate the regulatory mechanisms underlying terpolymer synthesis and to optimize strain fitness and production efficiency, thereby obtaining stable P(3HB-*co*-LA-*co*-3HV) materials. On this basis, achieving tunable mechanical properties and low-molecular-weight advantages will provide significant value for medical and cosmetic applications.

REFERENCES

1. Owusu P. A. and Asumadu-Sarkodie S. (2016). A review of renewable energy sources, sustainability issues and climate change mitigation. *Cogent. Eng.* **3**:1167990. DOI:10.1080/23311916.2016.1167990
2. Wang M., Chen L., Zhang Z., et al. (2025). Recent advances in genome mining and synthetic biology for discovery and biosynthesis of natural products. *Crit. Rev. Biotechnol.* **45**:236–256. DOI:10.1080/07388551.2024.2383754
3. Del Hierro A. G., Moreno-Cid J. A. and Casey E. (2024). Continuous biomanufacturing for sustainable bioeconomy applications. *EFB. Bioeconomy. J.* **4**:100071. DOI:10.1016/j.bioeco.2024.100071
4. Neto A. S., Wainaina S., Chandolias K., et al. (2025). Exploring the potential of syngas fermentation for recovery of high-value resources: A comprehensive review. *Curr. Pollut. Rep.* **11**:7. DOI:10.1007/s40726-024-00337-3
5. Hwang S., Joung C., Kim W., et al. (2023). Recent advances in non-model bacterial chassis construction. *Curr. Opin. Syst. Biol.* **36**:100471. DOI:10.1016/j.coisb.2023.

100471
6. Ye J. W. and Chen G. Q. (2021). *Halomonas* as a chassis. *Essays Biochem.* **65**:393–403. DOI:10.1042/EBC20200159
7. Dalton B., Bhagabati P., De Micco J., et al. (2022). A review on biological synthesis of the biodegradable polymers polyhydroxyalkanoates and the development of multiple applications. *Catalysts* **12**:319. DOI:10.3390/catal12030319
8. Fukala I. and Kučera I. (2024). Natural polyhydroxyalkanoates-An overview of bacterial production methods. *Molecules* **29**:2293. DOI:10.3390/molecules29102293
9. Chen X., Li M. and Chen G. Q. (2021). Thirty years of metabolic engineering for biosynthesis of polyhydroxyalkanoates. *Chin. J. Biotechnol.* **37**:1794–1811. DOI:10.13345/j.cjb.200457
10. Zhou W., Bergsma S., Colpa D. I., et al. (2023). Polyhydroxyalkanoates (PHAs) synthesis and degradation by microbes and applications towards a circular economy. *J. Environ. Manage.* **341**:118033. DOI:10.1016/j.jenvman.2023.118033
11. Yan X., Liu X., Yu L.P., et al. (2022). Biosynthesis of diverse α,ω-diol-derived polyhydroxyalkanoates by engineered *Halomonas bluephagenesis*. *Metab. Eng.* **72**:275–288. DOI:10.1016/j.ymben.2022.04.001
12. Jiang X.R. and Chen G.Q. (2016). Morphology engineering of bacteria for bio-production. *Biotechnol. Adv.* **34**:435–440. DOI:10.1016/j.biotechadv.2015.12.007
13. Wang H., Ouyang Y., Yang W., et al. (2025). Production and characterization of copolymers consisting of 3-hydroxybutyrate and increased 3-hydroxyvalerate by β-oxidation weakened *Halomonas*. *Metab. Eng.* **89**:97–107. DOI:10.1016/j.ymben.2025.02.009
14. Tang H. J., Neoh S. Z. and Sudesh K. (2022). A review on poly(3-hydroxybutyrate-*co*-3-hydroxyhexanoate) [P(3HB-*co*-3HHx)] and genetic modifications that affect its production. *Front. Bioeng. Biotechnol.* **10**:1057067. DOI:10.3389/fbioe.2022.1057067
15. Wen R., Chen Y., Wang J., et al. (2026). Pilot production of P(3HB-*co*-4HB) by engineered *Halomonas bluephagenesis* harboring an endogenous plasmid grown on glucose. *Metab. Eng.* **94**:153–168. DOI:10.1016/j.ymben.2025.11.017
16. Aversa C., Barletta M. and Koca N. (2023). Processing PLA/P(3HB)(4HB) blends for the manufacture of highly transparent, gas barrier and fully bio - based films for compostable packaging applications. *J. Appl. Polym. Sci.* **140**:e53669. DOI:10.1002/app.53669
17. Râpă M., Stefan L. M., Seciu-Grama A.M., et al. (2022). Poly(3-hydroxybutyrate-*co*-3-hydroxyvalerate) (P(3HB-*co*-3HV))/bacterial cellulose (BC) biocomposites for potential use in biomedical applications. *Polymers* **14**:5544. DOI:10.3390/polym14245544
18. Turco R., Santagata G., Corrado I., et al. (2021). In vivo and post-synthesis strategies to enhance the properties of PHB-based materials: A review. *Int. J. Biol. Macromol.* **8**:619266. DOI:10.3389/fbioe.2020.619266
19. Farah S., Anderson D. G. and Langer R. (2016). Physical and mechanical properties of PLA, and their functions in widespread applications — A comprehensive review. *Adv. Drug. Deliv. Rev.* **107**:367–392. DOI:10.1016/j.addr.2016.06.012
20. Poltronieri P. and Kumar P. (2019). Polyhydroxyalkanoates (PHAs) in industrial applications. *Handb. Ecomater.* **14**:2843–2872. DOI:10.1007/978-3-319-48281-1_70-1
21. Suhazsini P., Keshav R., Narayanan S., et al. (2020). A study on the synthesis of poly (3-hydroxybutyrate-*co*-3-hydroxyvalerate) by bacillus megaterium utilizing cheese whey permeate. *J. Polym. Environ.* **28**:1390–1405. DOI:10.1007/s10924-020-01687-x
22. Shozui F., Matsumoto K., Nakai T., et al. (2010). Biosynthesis of novel terpolymers poly(lactate-*co*-3-hydroxybutyrate-*co*-3-hydroxyvalerate)s in lactate-overproducing mutant *Escherichia coli* JW0885 by feeding propionate as a precursor of 3-hydroxyvalerate. *Appl. Microbiol. Biotechnol.* **85**:949–954. DOI:10.1007/s00253-009-2100-y
23. Yang F., Wang H., Zhao C., et al. (2024). Metabolic engineering of *Halomonas bluephagenesis* for production of five carbon molecular chemicals derived from L-lysine. *Metab. Eng.* **81**:227–237. DOI:10.1016/j.ymben.2023.12.001
24. Tan D., Xue Y.-S., Aibaidula G., et al. (2011). Unsterile and continuous production of polyhydroxybutyrate by *Halomonas* TD01. *Bioresour. Technol.* **102**:8130–8136. DOI:10.1016/j.biortech.2011.05.068
25. Chen Y., Chen X.Y., Du H.T., et al. (2019). Chromosome engineering of the TCA cycle in *Halomonas bluephagenesis* for production of copolymers of 3-hydroxybutyrate and 3-hydroxyvalerate (PHBV). *Metab. Eng.* **54**:69–82. DOI:10.1016/j.ymben.2019.03.006
26. Ye J., Hu D., Yin J., et al. (2020). Stimulus response-based fine-tuning of polyhydroxyalkanoate pathway in *Halomonas*. *Metab. Eng.* **57**:85–95. DOI:10.1016/j.ymben.2019.10.007
27. Yan X., Liu X., Yu L. P., et al. (2022). Biosynthesis of diverse α,ω-diol-derived polyhydroxyalkanoates by engineered *Halomonas bluephagenesis*. *Metab. Eng.* **72**:275–288. DOI:10.1016/j.ymben.2022.04.001
28. Chen Y. L., Liu X., Zhang L. Z., et al. (2025). Cell sizes matter for industrial bioproduction, a case of polyhydroxybutyrate. *Adv. Sc.* **2025**:2412256. DOI:10.1002/advs.202412256
29. Wang H., Ye J.W., Chen X., et al. (2023). Production of PHA copolymers consisting of 3-hydroxybutyrate and 3-hydroxyhexanoate (PHBHHx) by recombinant *Halomonas bluephagenesis*. *Chem. Eng. J.* **466**:143261. DOI:10.1016/j.cej.2023.143261
30. Wang H., Ouyang Y., Yang W., et al. (2025). Production and characterization of copolymers consisting of 3-hydroxybutyrate and increased 3-hydroxyvalerate by β-oxidation weakened *Halomonas*. *Metab. Eng.* **89**:97–103. DOI:10.1016/j.ymben.2025.02.009
31. Gibson D. G., Young L., Chuang R.-Y., et al. (2009). Enzymatic assembly of DNA molecules up to several hundred kilobases. *Nat. Methods* **6**:343–345. DOI:10.1038/nmeth.1318
32. Qin Q., Ling C., Zhao Y., et al. (2018). CRISPR/Cas9 editing genome of extremophile *Halomonas spp*. *Metab. Eng.* **47**:219–229. DOI:10.1016/j.ymben.2018.03.018
33. Wang L.J., Jiang X.R., Hou J., et al. (2022). Engineering *Halomonas bluephagenesis* via small regulatory RNAs. *Metab. Eng.* **73**:58–69. DOI:10.1016/j.ymben.2022.06.005
34. Simon R., Priefer U. and Puhler A. (1983). A broad host mobilization system for in vivo genetic engineering: Transposon mutagenesis in Gram-negative bacteria. *Bio/Technology* **1**:37–45. DOI:10.1038/nbt1183-784
35. Zhao H., Zhang H. M., Chen X., et al. (2017). Novel T7-like expression systems used for *Halomonas*. *Metab. Eng.* **39**:128–140. DOI:10.1016/j.ymben.2016.11.007
36. Silva-Rocha R., Martínez-García E., Calles B., et al. (2013). The standard European vector architecture (SEVA): A coherent platform for the analysis and deployment of complex prokaryotic phenotypes. *Nucleic Acids Res.* **41**:D666–D675. DOI:10.1093/nar/gks1119
37. Steinbuchel A. and Lutke-Eversloh T. (2003). Metabolic engineering and pathway construction for biotechnological production of relevant polyhydroxyalkanoates in microorganisms. *Biochem. Eng. J.* **16**:81–96. DOI 10.1016/S1369-703X(03)00036-6.
38. Chen G.Q. (2012). New challenges and opportunities for industrial biotechnology. *Microb. Cell Fact.* **11**:111. DOI:10.1186/1475-2859-11-111
39. Huo K., Zhao F., Zhang F., et al. (2020). Morphology engineering: A new strategy to construct microbial cell factories. *World. J. Microbiol. Biotechnol.* **36**:127. DOI:10.1007/s11274-020-02903-5
40. Kalia V. C., Patel S. K. S., Karthikeyan K. K., et al. (2024). Manipulating microbial cell morphology for the sustainable production of biopolymers. *Polymers* **16**:410. DOI:10.3390/polym16030410
41. Figge R. M., Divakaruni A. V. and Gober J. W. (2004). MreB, the cell shape-determining bacterial actin homologue, co-ordinates cell wall morphogenesis in *Caulobacter crescentus*. *Mol. Microbiol.* **51**:1321–1332. DOI:10.1111/j.1365-2958.2003.03936.x
42. Reid A. J., Erickson K. M., Hazel J. M., et al. (2023). Chemoenzymatic preparation of a campylobacter jejuni lipid-linked heptasaccharide on an azide-linked polyisoprenoid. *ACS Omega* **8**:15790–15798. DOI:10.1021/acs.biochem.6c00056
43. Zheng S., Zhang Z., Jiang P., et al. (2024). A self-stimulating system based on a polyhydroxyalkanoates coupled induction mechanism and its applications for *Halomonas*. *Chem. Eng. J.* **489**:151413. DOI:10.1016/j.cej.2024.151413

FUNDING AND ACKNOWLEDGMENTS

This study was supported by National Key Research and Development Program of China (Grant No. 2025YFA0921800), the National Nature Science Foundation of China (Grant No. 32130001) as well as the Center of Life Sciences of Tsinghua-Peking University. SEVA plasmids were kindly donated by Prof Victor de Lorenzo of Centro Nacional de Biotecnologia, CSIC/Spain. The funders had no role in study design, data collection and analysis, decision to publish, or preparation of the manuscript.

AUTHOR CONTRIBUTIONS

Jiangnan Chen: Conceptualization, Data analysis, Validation, Investigation, Visualization, Methodology, Software, Data Curation, Writing-original draft. Huan Wang: Data analysis, Validation, Investigation, Methodology, Data curation, Software. Zhenghao Xu: Methodology. Yiling Chen: Methodology. Shi Mu: Validation, Data analysis, Validation. Shaowei Li: Methodology. Fuqing Wu：Validation, Data analysis. Fang Yang: Conceptualization, Data analysis, Visualization, Investigation, Methodology, Data curation, Software, Writing-original draft. Guo-Qiang Chen: Conceptualization, Resources, Supervision, Funding acquisition, Writing original draft, Revision, Data analysis, Validation. All authors contributed to the manuscript and approved the final version.

DECLARATION OF INTERESTS

The authors declare no competing interests.

ETHICAL STATEMENT AND PATIENT CONSENT

No ethical approval or patient informed consent is required for this study, as no human participants or clinical samples were involved in the present research. See The Innovation website for more information.

DATA AND CODE AVAILABILITY

Data are available from the corresponding author upon reasonable request.

SUPPLEMENTAL INFORMATION

It can be found online at https://doi.org/10.59717/j.xinn-life.2026.100227.